# Energy metabolism and survival of the juvenile recruits of the American lobster (*Homarus americanus*) exposed to a gradient of elevated seawater $pCO_2$

**List of Authors**: Kayla Menu-Courey[1], Fanny Noisette[1,2], Sarah Piedalue[1], Dounia Daoud[3,4], Tammy Blair[5,6], Pierre U. Blier[1], Kumiko Azetsu-Scott[6], Piero Calosi[1]

[1] Département de Biologie, Chimie et Géographie, Université du Québec à Rimouski, 300 Allée des Ursulines, Rimouski, Québec, G5L 3A1, Canada.
[2] Institut des Sciences de la Mer, Université du Québec à Rimouski, 310 Allée des Ursulines, Rimouski, QC G5L 3A1, Canada
[3] Homarus Inc, 408 rue Main, Shediac, N-B E4P 2G1, Canada / EcoNov Inc., 540 Ch. Gorge Road, Moncton, NB, E1G 3H8
[4] EcoNov Inc., 540 Ch. Gorge Rd., Moncton, NB, E1G 3H8
[5] Fisheries and Oceans Canada, Saint Andrews Biological Station, 125 Marine Science Dr, Saint Andrews, N-B E5B 0E4, Canada.
[6] Fisheries and Oceans Canada, Bedford Institute of Oceanography, PO Box 1006, Dartmouth, NS B2Y 4A2, Canada.

Corresponding author: Piero Calosi, piero_calosi@uqar.ca

Key words: Ocean acidification, Carbon Capture and Storage, $CO_2$ leakages, fisheries, metabolic rate, mitochondria, crustacean, energy metabolism, mineralization, moult.

Paper Type: Research article

Short title: Juvenile American lobsters under elevated $pCO_2$

**ABSTRACT**

The transition from the last pelagic larval stage to the first benthic juvenile stage in the complex life cycle of marine invertebrates, such as the American lobster *Homarus americanus,* a species of high economic importance, represents a delicate phase in these species development. Under future elevated $pCO_2$ conditions, ocean acidification and other elevated $pCO_2$ events can negatively affect crustaceans. This said their effects on the benthic settlement phase are virtually unknown. This study aimed to identify the effects of elevated seawater $pCO_2$ on stage V American lobsters exposed to seven $pCO_2$ levels. The survival, development time, metabolic and feeding rates, carapace composition, and mitochondrial function were investigated. Results suggested an increase in mortality, slower development and a reduction in energetic capacity with increasing $pCO_2$. Our study points to potential reduction in juvenile recruitment success as seawater $pCO_2$ increases, thus foreshadowing important socio- economic repercussions for the lobster fisheries and industry.

Key words: Ocean acidification, Carbon Capture and Storage, $CO_2$ leakages, fisheries, metabolic rate, mitochondria, crustacean, energy metabolism, mineralization, moult.

## 1. INTRODUCTION

Up to 85 % of all benthic marine species possess complex life cycles (CLC) with distinct larval stages preceding metamorphosis to the juvenile stages that lead to the adult phase (Pechenik, 1999). Relevant examples exist across multiple phyla, such as molluscs, echinoderms, and decapod crustaceans (Eckstrom *et al*., 2015). Commercially important crustacean species, namely shrimps, crabs and lobsters, have CLC that include several developmental stages, associated to distinct habitat occupations, characterised by distinctive morphological, physiological, and behavioural traits (Charmantier et al. 1991; Factor, 1995; Spicer and Eriksson, 2003; Spicer and Gaston 1999). Among these crustaceans, the American lobster, *Homarus americanus* (H. Milne Edwards, 1837), possesses three pelagic larval stages followed by an intermediate post-larval stage that eventually settle on the benthos, marking the success of juvenile recruitment (Incze and Wahle, 1997). The metamorphic moult to the post-larval stage (stage IV) represents a pivotal transition between the larval pelagic phase and the juvenile benthic phase (Factor, 1995; Wahle and Steneck, 1991; Whale 2003). It is critical for recruitment success for the stage IV post-larvae to settle and successfully moult to the stage V, considered as the first juvenile stage (Incze and Wahle, 1997). The first stages of lobster recruitment have naturally high mortality rates, being known to represent a bottleneck in the lobsters' life cycle (Wahle and Stenneck ,1991). The number of benthic recruits, ultimately contributing to the adult population, defines the future viability of natural populations and the sustainability of stocks, particularly when under harvesting pressure (Steneck and Wilson, 2001; Wahle and Stenneck, 1991).

With the lobster landed value's progressive growth to over $ 1,2 billion just in 2016 in Atlantic Canada according to Fisheries and Oceans Canada (http://www.dfo-mpo.gc.ca/stats/commercial/sea-maritimes-eng.htm), and landings reaching record highs above 40 000 million tonnes in the USA in the early 2000's (Wahle *et al.,* 2011), the Canadian and American lobster industries prioritize the protection of this resource after seeing record-breaking population declines in the early 2000's in some regions along the coast of both countries (Comeau *et al.,* 2004; Stenneck and Wilson 2001). Since benthic recruitment begins with the successful settlement of stage IV post-larvae, the release of individuals during this developmental stage has become a popular method in an attempt to increase recruitment and future stock abundances (e.g. Bannister and Addison, 1998; Castro *et al.,* 2001; Comeau *et al.,* 2004). Within the context of a rapidly changing and often degrading environment, as the consequence of human activities in coastal areas, the viability of natural populations and harvested stock may however be under threat in some areas (Cheung *et al*., 2010). Whilst the impacts of global warming are already relatively well known on the American lobster (e.g. Chiasson *et al.*, 2015; Drinkwater *et al*., 2006), the investigation of the potential impact of low pH/elevated $pCO_2$ conditions on this species is still in its beginning phase (Caputi *et al*., 2013, Waller *et al*., 2016, McLean *et al*., 2018). This is particularly important for the critical early life stages in nature (Waller *et al.,* 2016), and even more so for the survival of post-larval (stage IV) individuals released into the wild for stock enhancement (Addison and Bannister, 1994).

It is therefore important to better understand the potential impacts of emerging global change drivers (IPCC 2014), such as ocean acidification (OA) and other extreme elevated $pCO_2$ events (e.g. extreme coastal events and leakages from carbon capture storage (CCS) systems), on the survival of this economically important species.

Ocean acidification is the result of anthropogenic atmospheric $CO_2$ uptake since the beginning of the industrial revolution, leading to an increase in seawater $pCO_2$ and $[HCO_3^-]$, and a lowering in seawater pH and $[CO_3^{2-}]$ (Zeebe and Wolf-Gladrow, 2001; IPCC, 2014). According to the IPCC (2014) under RCP 8.5 climate scenario, an increase in atmospheric $CO_2$ to approx. 500 ppm by 2050 and 1000 ppm by 2100 will correspond to a drop in the open ocean pH to 7.95 and 7.75 respectively (Pörtner *et al*., 2014). In coastal areas, pH fluctuations already go beyond average global predicted values for seawater pH and $pCO_2$ (Duarte *et al.,* 2013; Hoffman *et al*., 2011), as the result of many processes, such as coastal influx of freshwater and human-induced coastal eutrophication that causes high respiration in the water column and in the benthic communities (Waldbusser *et al*., 2013). Besides, the potential construction of CCS in our oceans, as an attempt to slow down the negative impact of climate changes (Blackford *et al.,* 2009; Blackford *et al.,* 2015), may represent a local driver for increase in seawater $pCO_2$ which may further affect marine benthic organisms in the case of accidental fissures in these systems (Blackford *et al.,* 2009; Donohue et al 2012; Small et al 2016; Widdicombe *et al.,* 2015). Furthermore, oceanic currents and stratification can easily trap water masses rich in $CO_2$ produced by a CCS leak (Phelps *et al.,* 2015), making the construction of these facilities a serious risk and an additional threat to marine biodiversity and ecosystem functioning (Blackford *et al*., 2015; Christen *et al.* 2013).

Our aim was to investigate the effects of the exposure of post-larval (stage IV) of the American lobster to a seven-level gradient of elevated seawater $pCO_2$ on the life history and physiological traits of the next life stage: stage V, the first juvenile stage. Seawater $pCO_2$ conditions tested here ranged from current to future seawater $pCO_2$ scenarios occurring in coastal areas and estuaries, as well as future OA conditions, and CCS leakages. Post-larval stage IV individuals of the American lobster were raised in seven $pCO_2$ levels in order to observe the implications of pre-exposition throughout the moult process on the stage V juveniles. Survival, development, structure, metabolism, feeding rates, and energetics of the juvenile lobsters were measured along the experimental $pCO_2$ gradient. In addition, we characterised the vertical physical and chemical profiles of female lobster habitat parameters (i.e. temperature, pH, and salinity) *in situ* over the locality from which berried females had been collected (Shediac station, NB, Canada), in order to help developing the discussion of our laboratory experiment results, whilst improving our understanding of the natural $pCO_2$ profiles experienced by lobsters.

## 2. MATERIALS AND METHODS

### 2.1 Physical and chemical characterisation of lobster habitat

Vertical physical and chemical profiles of female lobster habitat parameters (i.e. temperature, pH, and salinity) were measured directly from nine daily *in situ* seawater samples over in Shediac station (NB, Canada) using a Conductivity-Temperature-Depth (CTD) oceanographic sensor. Seawater samples were collected in 500 mL borosilicate bottles, poisoned with a saturated solution of $HgCl_2$ and stored before being analyzed, following standard operating procedures described in Dickson et al. (2007). Stored samples were analyzed within three months of collection. The dissolved inorganic carbon (DIC) was determined using gas extraction from an acidified sample with a coulometric quantification of the $CO_2$ released (Johnson et al., 1985). The total alkalinity (TA) was determined by open-cell potentiometric titration with a five-point method (Haradsson et al., 1997). Certified Reference Material supplied by Professor Andrew Dickson, Scripps Institution of Oceanography, San Diego, USA, was analyzed in duplicate every 20 samples for accuracy. CTD-pH measurements were calibrated against pH values that were calculated from DIC and TA measurements from water samples. Since only nine water samples per profile were collected, the relationship between total alkalinity and salinity was calculated for each year between 2012 and 2016 in order to get total alkalinity profiles. The $pCO_2$ and saturation states were then calculated using pH and total alkalinity.

### 2.2 Specimen collection, transport and maintenance

Lobstermen from the Maritimes Fishermen's Union captured egg-bearing female lobsters (*H. americanus;* H. Milne Edwards, 1837) using benthic lobster traps off the coast of the Acadian peninsula (NB, Canada) in the Baie des Chaleurs of the Northumberland Strait (47°46'47"N 64°42'49"W) in May 2016. Ovigerous females were held on land in highly aerated 500 L tanks supplied with mechanically and biologically filtered seawater from the Baie des Chaleurs (T = 20 °C, pH = 8.0, salinity = 28) at the Homarus Inc.-Coastal Zones Research Institute (Shediac, NB). Hatched individuals were transferred to 20 L kreissels containing recirculated mechanically and biologically filtered seawater and fed frozen *Artemia* (Hikari, Kyorin Co. Ltd, Kanschai City, Japan) twice daily. Larvae were reared communally to the stage IV. Immediately after moulting to stage IV, 2 000 stage IV post-larval lobsters (considered 0 days (d) old for this experiment) were transported by car in aerated coolers (Coleman 48-Quart Cooler, Brampton, ON, Canada) to Fisheries and Oceans Canada's Biological Station laboratory in Saint Andrews (NB, Canada) within 6 h. Seawater conditions were monitor during transport to be maintained as stable as possible around culturing conditions.

### 2.3 Experimental design and $CO_2$ manipulation system

In order to test the impacts of post-larval exposure to elevated $pCO_2$ levels on the life history and physiology of juvenile lobsters, post-larval (stage IV) lobsters were exposed to a gradient of current and future $pCO_2$ scenarios. The latter were chosen based on current global ocean conditions (400 $\mu$atm) to predicted $pCO_2$ values between now and the end of the century (600, 800, 1 000 $\mu$atm, IPCC 2014), ecologically relevant coastal

$pCO_2$ fluctuations (1 200 $\mu$atm, Waldbusser & Salisbury 2013), and levels potentially achieved from industrial accidents involving carbon capture storage (CCS) leakages (2 000 and 3 000 $\mu$atm, Rastelli *et al.,* 2016).

Upon arrival, specimens were transferred gently and kept individually in basket-like containers that were 3.5“ in diameter (Net Pots, Canadian Wholesale Hypotonics, Elie, MN, Canada) rafted at the water surface of 500 L tanks (1 m diameter x 0.70 m depth), i.e. the replicate units of the different seawater $pCO_2$ levels. Post-larval stage IV lobsters were split into the 24 $CO_2$-enriched tanks, the elevated $pCO_2$ treatments, and the four control treatment tanks (without any $pCO_2$ regulation) with 15 indiv. *per* tank, corresponding to 60 indiv. *per* condition. Four replicate 500 L tanks *per* $pCO_2$ level were used. Within the 72 h following transfer, dead individuals were replaced before testing the biological effects of post-larval exposure at elevated $pCO_2$ levels on stage V juvenile lobsters.

Incoming water entering the two header tanks responsible for filling each experimental tank was supplied from Brandy Cove in the Passamaquoddy Bay (NB, Canada), passing through a series of sand filters (20 $\mu$m), a UV-treatment, heated at 18 °C, mimicking the optimal temperature for growth and survival of juvenile lobster from Baie des Chaleurs in the laboratory (Daoud *et al.,* 2014) and bubbled with ambient air. Header tanks were bubbled with ambient air to oxygenate incoming seawater. Daily measurements of salinity (see next section for daily measurements) remained relatively constant throughout the experiment at 31.5 (± 0.02) on average.

The $pCO_2$ treatments were maintained using a pH regulation system (IKS, AquaStar, Karlsbad, Germany) equipped with a glass electrode per tank to measure pH every 5 min. From the measured pH in each tank, the IKS system individually released $CO_2$ gas into the seawater, maintaining the desired pH level for all six conditions tested in this study. IKS pH levels were calibrated daily from independent pH measurements made in each of the tanks (see next section for daily measurements) Furthermore, all tanks were air bubbled to maintain oxygen saturation and equipped with a water pump (Maxi-Jet 400, Marineland Aquarium Products, Cincinnati, OH, USA) to facilitate water mixing and to maintain homogeneous water chemistry within the tanks.

### 2.4 Physical and chemical monitoring and characterisation of seawater in the laboratory experiment

Seawater physical and chemical parameters (i.e. temperature, salinity, pH on the total scale ($pH_T$), and dissolved oxygen) were monitored daily over the duration of the experiment using a pH meter (SevenGo Portable pH Meter, Mettler Toledo, Mississauga, ON, Canada) calibrated with Tris HCl buffer (Dickson *et al.*, 2007) and an oxygen meter (SevenGo Portable Dissolved Oxygen Meter, Mettler Toledo). Over the course of the experiment, water samples were collected weekly in each treatment for TA, DIC, and pH measurements following the method described above. The carbonate chemistry (i.e. $pCO_2$, $[HCO_3^-]$, $[CO_3^-]$, DIC, $\Omega_{ara}$, $\Omega_{cal}$) of the seawater in each pH / $pCO_2$ condition (Table 1) was calculated in R (version 3.0.1) using the “Seacarb” package (Gattuso *et al.,* 2015) by combining the average weekly alkalinity and salinity with daily measurements of temperature (T °C) and $pH_T$ made over the course of the experiment.

For the laboratory experiment, detailed measurements and calculated values of the physico-chemical seawater parameters are depicted in Table 1 below. Salinity remained constant in all tanks throughout the experimental period at 31.5 ± 0.02 units, temperature remained constant in all quadruplicates of the seven $pCO_2$ treatments (between 17.97 ± 0.014 and 18.12 ± 0.089 °C), and DO remained constant n all quadruplicates of the seven pCO2 treatments (between 98.14 ± 1.2 and 109.1 ± 0.8 %). The pH and $pCO_2$ for each treatment remained relatively constant throughout the course of the experiment, fluctuating slightly above or below the targeted level. The measured carbon species, such as $HCO_3^-$, $CO_3^-$, and DIC remained relatively constant throughout the course of the experiment, with little variation. Measured TA levels were constant throughout each experimental tank, with very little variation between treatments. Calculated omega ratio for aragonite and calcite were well above saturation levels between 400 and 1 200 $\mu$atm $pCO_2$ treatments, and under-saturated at the 2 000 and 3 000 $\mu$atm $pCO_2$ level.

**2.5 Determination of survivorship and development periods**

Individual lobsters were checked daily to record mortalities and evidence of a stage change (e.g. shed carapace). Dead individuals were removed immediately to avoid bacterial accumulation and contamination in the tanks. The moulting date presumed for stage IV lobsters was the same day as their arrival. The intermoult period to the stage V moult (IP) was then determined in number of days using the following formula:

(Eq. 1) $$IP = M_{IV} - M_V$$

Where $M_{IV}$ is the moulting date at stage IV and $M_V$ is the moulting date to stage V observed in the experimental tanks

**2.6 Determination of feeding rates and routine metabolic rates**

Routine metabolic rates (RMR), defined here as oxygen consumption rates during rest activity when lobsters are mostly immobile and not disrupted by light, noise, or physical disturbances, were used as proxies of metabolism for the juvenile lobsters at stage V across pH/ $pCO_2$ condition. Feeding rates (FR) and RMR were determined for each $pCO_2$ condition in eight (i.e. two *per* tank) freshly moulted stage V individuals, which moulted the same day, *per* seawater condition.

In order to determine FR, individuals were not fed for 24 h and then fed pre-weighed and seawater-soaked blocks of herring, *Clupea harengus*, as their food. Non-ingested food was removed and immediately weighed after 1 h in the containers with each selected individual in order to calculate the FR per individual as mg $h^{-1}$ g wet body $mass^{-1}$ as follows:

(Eq. 2) $$FR = \frac{\Delta \mathrm{H}}{WBM \times \Delta t}$$

Where Δ H is the mass (mg) of consumed herring, WBM is the wet body mass (g) for each individual stage V juvenile lobster, and Δ t is the elapsed time during food consumption.

Hereafter, the same individuals were deprived of food again for 24 h removing digestion bias on the metabolism in preparation for the determination of RMR (Speakman and McQueenie, 1996). Following this procedure, individuals in each tank were then carefully placed in 16 mL borosilicate glass vials (Vials w/ Cap 1.5 drams, VWR International Ltd, Ville Mont-Royal, QC, Canada). Vials were sealed with mesh and rubber bands in order to prevent the lobsters from escaping, while allowing for sufficient water flow in the vial during a 12 h period. During this time, the lobster could adjust to the vial, thus reducing stress from the handling and introduction to the new environment. One control vial *per* $pCO_2$ condition was used to investigate the potential microbial respiration in the seawater. These contained seawater from the tested tank and were manipulated identically to all other vials. Following the 12 h adjustment period, the mesh was replaced by lids in order to seal the vials with the appropriate seawater $pCO_2$ as in the corresponding experimental tanks. The vials containing both juveniles and the blank samples were moved using an 18 °C water bath to an infrared-illuminated, temperature-controlled room at 18 °C. Each vial was equipped with a stirring rod that was isolated from the lobsters by a mesh to ensure homogenous oxygen concentrations throughout the vials once sealed shut. All sealed vials were kept in water basins over magnetic stirrer plates (Mix 15, 2Mag AG, Munich, Germany) to activate stirrers in each vial, thus the mixture of the internal seawater.
Preliminary trials showed linear oxygen consumption above 70 % $O_2$ saturation, and RMR measurements were stopped before reaching such limit. $O_2$ concentration ($\mu$mol $L^{-1}$) were measured using a non-invasive fiber-optic system (Fibox 4, PreSens, Regensburg, Germany) composed of an optical fiber, a temperature probe and reactive oxygen sensor spots glued inside the vials and calibrated according to the manufacturer instructions with 0 and 100 % buffers. Measurements were recorded at the beginning and end of the incubation period as the oxygen consumption has been proved linear. RMR ($\mu$mol $O_2$ $h^{-1}$) for individual stage V juvenile lobsters was calculated following the Eq. 2 and corrected by the blank control vials to remove oxygen consumption due to microbial activity.

(Eq. 2) $$RMR_{vial} = \frac{\Delta O_2 \times V}{\Delta t}$$

Where $RMR_{vial}$ is the oxygen consumption inside the vial, Δ $O_2$ is the difference between the initial and final [$O_2$] ($\mu$mol $O_2$ $h^{-1}$), V is the volume of the vial (L), and Δ t is the incubation time (h) for each individual stage V juvenile lobster.

After each measure, the lobster was photographed using a binocular (M80, Leica Microsystems GmbH, Wetzlar, Germany) under at magnification x7.5 with a picture

acquisition system (IC80 HD, Leica Microsystems GmbH) for morphometric measurements, blotted dry with wipes (KimWipe, Kimtech Science, Brampton, ON, Canada) and weighed to obtain the wet body mass. They were then dissected using non-metal tools (White Plastic Tweezers, Swiss Precision Instrument Inc., Garden Grove, CA, USA) into two sections (cephalothorax and claws, and abdomen and telson), which were frozen and stored at - 80 °C using liquid nitrogen separately to preserve the carapace and tissues for further analyses.

**2.7 Determination of morphometrics**

Photographs of stage V juvenile lobsters used to determine for FR and RMR were analyzed using ImageJ Software (ImageJ 1.45s, National Institute of Health, Madison, WI, USA) to investigate effect of elevated $pCO_2$ on growth and body proportions. Seven morphological characteristic lengths were measured. The rostrum length (1), starting from behind the eye to the tip of the rostrum structure, the dominant claw's pollex (2), starting from the joint to the tip of the structure, and the dactylus (3), starting from the joint to the tip of the structure. The thorax length (4), from the junction to the abdomen to the junction with the rostrum, the abdomen length (5), starting from the junction of the first segment to the thorax to the tip of the last segment that joins with the telson. Finally, the telson length (6), starting at the junction with the abdomen to the tip of the structure was measured. The total lobster length was calculated from adding the measured lengths of structures 4, 5, and 6. The measurements of cephalothorax and abdomen lengths were also used in order to determine ratio changes of these two sections across pH/ $pCO_2$ conditions.

**2.8 Determination of carapace mineral content**

The effects of low $pCO_2$ levels on carapace mineral content were determined using the whole cephalothorax carapace of all stage V juvenile lobsters at all $pCO_2$ conditions. Chemical analyses on the carapace of the stage V juvenile lobsters were performed at the Laboratoire de Chimie Marine et Spectrométrie de Masse at the Institut des Sciences de la Mer de Rimouski (ISMER) at the University of Quebec in Rimouski (Rimouski, Canada). Previously frozen cephalothorax carapace samples were removed from the rest of the upper body using plastic dissection tools (White Plastic Tweezers, Swiss Precision Instrument Inc.) to avoid element contamination from metal tools and freeze dried (T = -50 °C) for 12 h to remove any residual moisture (Freezone Freeze Dry Systems, Labcono, Kansas City, MO, USA). Samples were then weighed on a high precision microbalance (MX5 Analytical Micro-balance, Mettler Toledo). Hereafter, they were digested in a mixture of pure nitric acid and peroxide hydrogen (375 µL : 125 µL) (TraceSelect grade, Sigma Aldrich, St. Louis, MO, USA) at room temperature for 24 h and after short periods warming in a water bath. Samples diluted in ultrapure water were analyzed by inductively coupled plasma (ICP) interfaced to a quadruple mass spectrometer (MS - ICP-MS, Agilent 7500c with micro flow nebulizer, Agilent Technologies, Santa Clara, CA, USA) equipped with an autosampler (ASX 520, Teledyne CETAC, Omaha, NB, USA). Element signals were acquired for 200 msec *per* mass, and three acquisitions were realized. Element quantification ($[Sr^{2+}]$, $[Ca^{2+}]$, $[Mg^{2+}]$, $[Na^{+}]$, and

[$K^+$]) was performed in normal mode with a ten-point external calibration using multi-element reference material (Multi-Element 5, Sigma Aldrich, St. Louis, MO, USA) with a concentration range between 0.10 and 50 for [$Sr^{2+}$] and 1.00 and 500 ng $mL^{-1}$ for other elements. Performances of the method and instrument stability were assessed repeatedly by the analysis of a quality control solution of known metal concentration during the course of analysis coupled with a procedural blank. Control of the system, acquisition and data processing were carried out with the Agilent ChemStation software (Agilent Technologies).

**2.9 Assays of energy metabolism enzymes**

Frozen abdomen tissues of the same sampled individuals used for carapace mineral content were used to determine enzymatic activities. Lactate dehydrogenase (LDH) and the Electron Transport System (ETS) activities were measured in order to infer anaerobic (LDH) and aerobic (ETS) responses or adjustments to environmental conditions All solutions used were mixed following the protocol from Thibeault *et al*. (1997) for LDH activity and from Lanning *et al*. (2003) for ETS activity. Frozen abdomen tissues were separated from the carapace in a polystyrene petri-dish, weighed, crushed, and diluted in one parts tissue and 50 parts 100 mM potassium phosphate buffer at pH 7.0 and 8.5 for LDH and ETS, respectively, in two 2 mL microtubes over ice to create a homogenate tissue dilution. Duplicate wells for each individual lobster were mixed in a polystyrene well plate (96-Well Assay Microplate, Fisher Scientific) with reaction solutions for the LDH and ETS and passed through a well plate reader (2104 EnVision Multilabel Plate Reader, Perkin Elmer Inc, Waltham, MA, USA) providing the reaction slopes of the solution absorbance (at 340 and 490 nm, respectively). All well readings were performed at 18 °C to mimic seawater experimental conditions. LDH and ETS enzyme activities (U mg $protein^{-1}$) were calculated with the extinction coefficient of 6.22 mL $cm^{-1}$ $\mu mol^{-1}$ for NADH and 15.9 mL $cm^{-1}$ $\mu mol^{-1}$ INT.

Protein content was determined for each tissue dilution using the Bicinchoninic Acid Protein Assay Method (Krohn *et al.,* 1985) with BSA for a standard curve.

**2.10 Statistical analyses**

Best-fit curve approach, using as references the linear, logarithmic, two-order polynomial, three-order polynomial regressions types to optimize the representation of the trends observed, was used to determine the effect of exposure to increasing $pCO_2$ levels on the life history and physiological traits of stage V juvenile recruitment.

Data were first tested for the assumption of normal distribution with a Shapiro-Wilk test, and then verified for variance homogeneity using Levene's test. Once assumptions were met using a global model that included all measured variables throughout the experimental period, the random variable "tank", representing the four replicate tanks for each $pCO_2$ level tested, was analyzed in the complete model as a random factor, and removed in all cases because it was never found to be significant ($p > 0.05$). Three significant covariates ($p < 0.05$) were included in final models for most analyses to take into account differences between individuals and scientific methods: (1) wet body mass was used as a covariate for FR, RMR, and mineral quantification, (2) total body length

was used as a covariate for all morphological trait lengths except for the total body length and the cephalothorax-abdomen ratio, (3) temperature (recorded during the $O_2$ measurements) was used as a covariate for RMR. Out of the statistically different models ($P > 0.05$), the one with the best AIC and $R^2$ was selected as the final best-fit curve for each measured trait.

## 3. RESULTS

### 3.1 *In situ* physical and chemical profiles of lobster habitat

The physical environment in which post-larval American lobsters are present, between May and November, ranges from the surface to the seabed throughout the water column (Factor, 1995; Spicer et Eriksson, 2003; Whale, 2003; Whale and Steneck, 1991). The vertical profiles of temperature, salinity, $pH_T$, $pCO_2$, and seawater saturation states with respect to aragonite and calcite (omega), indicate that the environment in which stage IV post-larvae evolve is varying, and highly fluctuating (Fig. 1, Fig. 2) in time and depth.

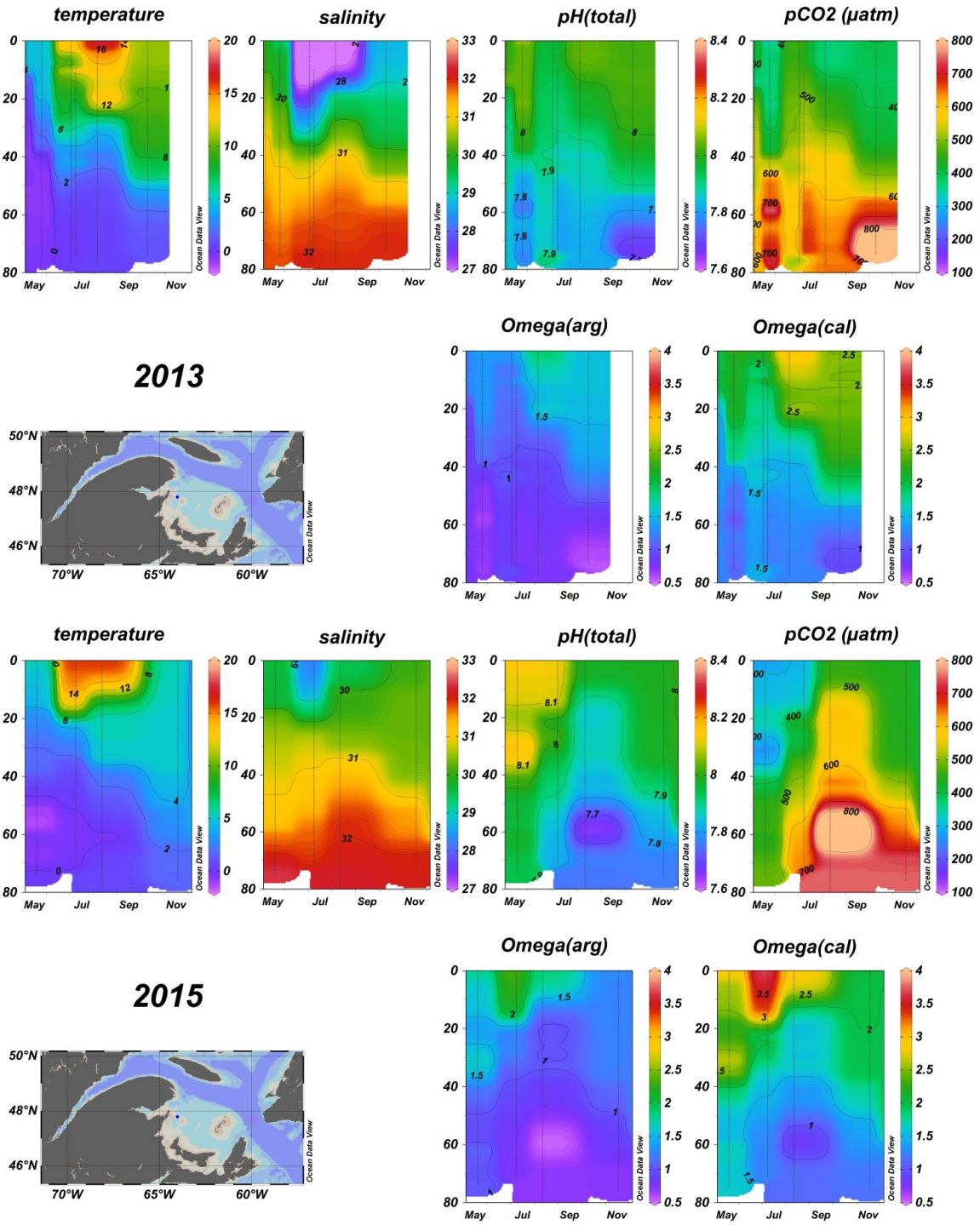


**Fig. 1.** Time series of physical and chemical seawater vertical profiles over the months of May to November, during which the highest abundance of post-larval (stage IV) and juvenile (stage V) American lobsters occur in the wild in this region. The vertical profiles of salinity (sal), and temperature (T °C) were obtained from *in situ* CTD-measurements, while the pH in the total scale ($pH_T$), $CO_2$ partial pressure: $pCO_2$ ($\mu$atm), saturation state

of seawater with respect to calcium ($omega_{cal}$), and saturation state of seawater with respect to aragonite ($omega_{ara}$) were calculated using total alkalinity (TA), dissolved inorganic carbon (DIC), and pH measurements from 2013 (top) and 2015 (bottom) seawater samples.

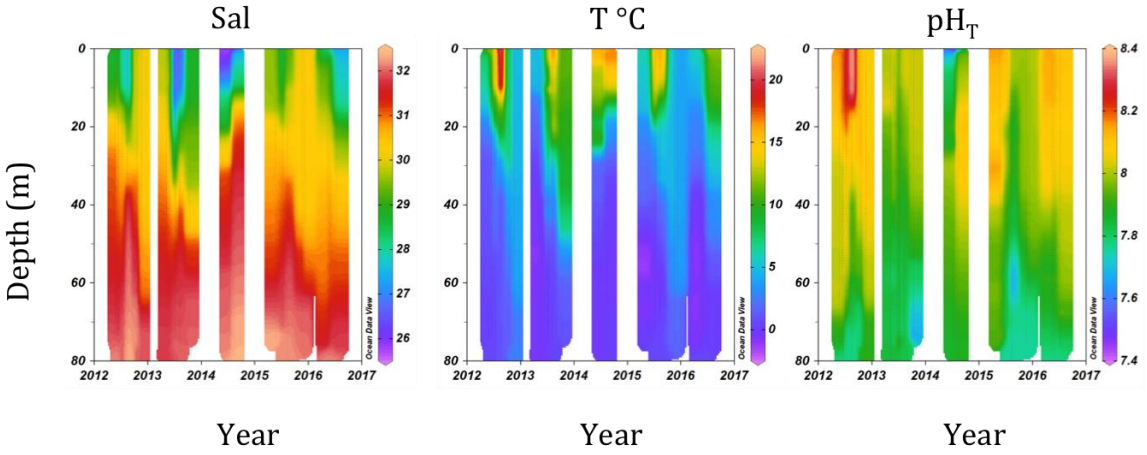


**Fig. 2.** Vertical profile of salinity, $pH_T$, and $omega_{cal, ara}$ time series over a period of four years (2012- 2016) obtained from *in situ* seawater CTD-measurements of salinity and temperature and laboratory calculations from total alkalinity (TA), dissolved inorganic carbon (DIC), and pH.

**Table 1** (*next page*). Mean (± SE) measured and calculated (indicated with an asterix *) seawater physico-chemical parameters in control and experimental conditions over the course of the experiment. The number of daily measurements: n, temperature: T, salinity: sal, DO: dissolved oxygen, pH in the total scale: $pH_T$, $CO_2$ partial pressure: $pCO_2$, bicarbonate ion concentration: $HCO_3^-$, carbonate ion concentration: $CO_3^-$, total dissolved inorganic carbon: DIC, total alkalinity: TA, saturation state of seawater with respect to aragonite: $\Omega_{ara}$, saturation state of seawater with respect to calcite: $\Omega_{cal}$.

437

| $pCO_2$ | 400 | 600 | 800 | 1000 | 1200 | 2000 | 3000 |
|---|---|---|---|---|---|---|---|
| **n** | **111** | **112** | **112** | **106** | **109** | **108** | **106** |
| **T (°C)** | 17.97± 0.012 | 18.10 ± 0.12 | 18.12 ± 0.089 | 18.08 ± 0.11 | 18.09± 0.11 | 17.97± 0.014 | 18.00± 0.012 |
| **Sal** | 31.5 ± 0.02 | 31.5 ± 0.02 | 31.5 ± 0.02 | 31.5 ± 0.02 | 31.5 ± 0.02 | 31.5 ± 0.02 | 31.5 ± 0.02 |
| **DO (%)** | 98.14 ± 1.2 | 98.48 ± 1.4 | 98.86 ± 1.1 | 108.1 ± 0.9 | 99.17 ± 0.9 | 109.1 ± 0.8 | 98.91 ± 0.9 |
| **$pH_T$** | 7.97 ± 0.02 | 7.89 ± 0.06 | 7.8 ± 0.10 | 7.73 ± 0.10 | 7.67 ± 0.10 | 7.39 ± 0.12 | 7.17 ± 0.11 |
| ***$pCO_2$ ($\mu$atm)** | 473.27 ± 2.63 | 586.42 ± 11.47 | 760.89 ± 22.35 | 912.31 ± 27.12 | 1047.97± 25.60 | 2116.89± 65.32 | 3513.59± 98.08 |
| ***$HCO_3^-$ ($\mu$mol $kg^{-1}$)** | 1815.917 ± 0.0211 | 1858.850 ± 2.617 | 1904.612 ± 3.536 | 1935.822 ± 3.662 | 1958.731 ± 3.391 | 2039.756 ± 2.028 | 2075.362 ± 1.764 |
| ***$CO_3^-$ ($\mu$mol $kg^{-1}$)** | 129.192 ± 0.576 | 111.878 ± 1.134 | 93.403 ± 1.530 | 80.733 ± 1.613 | 71.517 ± 1.466 | 38.797± 0.854 | 24.330 ± 0.672 |
| ***DIC ($\mu$mol $kg^{-1}$)** | 1961.605 ± 0.791 | 1991.037 ± 1.836 | 2024.367 ± 2.740 | 2048.187 ± 2.894 | 2066.558 ± 2.696 | 2152.344 ± 3.347 | 2222.062 ± 4.239 |

| | | | | | | | |
|---|---|---|---|---|---|---|---|
| ***TA** ($\mu$mol kg$^{-1}$) | 2135.872 ± 0.640 | 2135.896 ± 0.635 | 2135.896 ± 0.635 | 2135.743 ± 0.668 | 2135.822 ± 0.651 | 2135.796 ± 0.657 | 2135.524 ± 640 |
| ***Ω** $_{ara}$ | 2.028 ± 0.00895 | 1.758 ± 0.0176 | 1.467 ± 0.0239 | 1.268 ± 0.0252 | 1.123 ± 0.0230 | 0.609 ± 0.0134 | 0.382 ± 0.0106 |
| ***Ω** $_{cal}$ | 3.161 ± 0.0139 | 2.738 ± 0.276 | 2.285 ± 0.0373 | 1.975 ± 0.0393 | 1.750 ± 0.0358 | 0.949 ± 0.0209 | 0.595 ± 0.0164 |

454 **Table 2.** Mean (±SE) life history and physiological traits: survival rate, intermolt period (IP), feeding rate (FR), routine metabolic rate
455 (RMR), abdomen length (AL), cephalothorax length (CL), telson length (TL), cephalothorax-abdomen length ratio (CL : AL), carapace
456 [$Mg^{2+}$], and electron transport system – lactate dehydrogenase ratio of mitochondrial function (ETS : LDH) under seven $pCO_2$ levels
457 for stage V juvenile of the American lobster *Homarus americanus*.
458

| $pCO_2$ ($\mu$atm) | 400 | 600 | 800 | 1000 | 1200 | 2000 | 3000 |
|---|---|---|---|---|---|---|---|
| **Survival (%)** | 51.28 ± 8.11 | 60.52 ± 8.040 | 45.71 ± 8.54 | 50.00 ± 8.70 | 39.02 ± 7.71 | 37.84 ± 8.083 | 36.59 ± 7.62 |
| **IP (d)** | 17.69 ± 0.42 | 17.71 ± 0.39 | 18.41 ± 0.37 | 17.85 ± 0.40 | 17.73 ± 0.36 | 19.054 ± 0.36 | 19.051 ± 0.56 |
| **FR (mg $g^{-1}$ $h^{-1}$)** | 131.15 ± 32.72 | 153.03 ± 42.12 | 74.93 ± 24.50 | 199.33 ± 13.86 | NA | 241.19 ± 40.33 | 139.85 ± 33.18 |
| **RMR ($\mu$mol $h^{-1}$)** | 1.0647 ± 0.185 | 0.775 ± 0.0734 | 0.615 ± 0.141 | 0.705 ± 0.0699 | 0.791 ± 0.124 | 0.812 ± 0.152 | 0.767 ± 0.147 |
| **AL (mm)** | 5.467 ±0.230 | 5.504 ± 0.292 | 5.301 ± 0.295 | 5.0766 ± 0.247 | 4.923 ± 0.192 | 5.307 ± 0.316 | 5.0134 ± 0.260 |
| | 4.624 ± 0.183 | 4.644 ± 0.148 | 4.773 ± 0.147 | 4.651 ± 0.0778 | 4.638 ± 0.0546 | 5.0290 ± 0.161 | 4.848 ± 0.118 |

| | | | | | | | |
|---|---|---|---|---|---|---|---|
| **CL (mm)** | | | | | | | |
| **TL (mm)** | 2.898 ± 0.138 | 2.853 ± 0.110 | 2.964 ± 0.119 | 2.792 ± 0.151 | 2.661 ± 0.0510 | 2.598 ± 0.102 | 2.648 ± 0.123 |
| **CL : AL** | 0.856 ± 0.0569 | 0.852 ± 0.0361 | 0.909 ± 0.0277 | 0.928 ± 0.0349 | 0.948 ± 0.0307 | 0.958 ± 0.0535 | 0.979 ± 0.0411 |
| **[$Mg^{2+}$] (ng $mg^{-1}$)** | 16440 ±618 | 17772 ± 924 | 15977 ± 881 | 16756 ± 1056 | 18182 ± 765 | 19225 ± 1145 | NA |
| **ETS : LDH** | 0.718 ± 0.0698 | 0.775 ± 0.0384 | 0.844 ± 0.0503 | 0.892 ± 0.0514 | 1.237 ± 0.110 | 1.367 ± 0.0540 | NA |

460 **3.2 Survivorship and development periods**

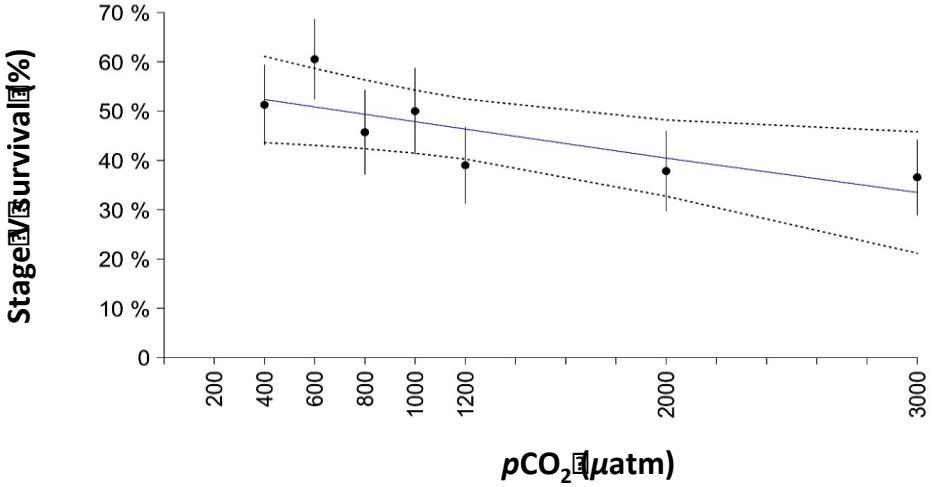


461 **Fig. 3.** Relationship between seawater $pCO_2$ levels (400, 600, 800, 1000, 1200, 2000,
462 3000 $\mu$atm) and survivorship of stage V juveniles of the American lobster, *Homarus*
463 *americanus* (± SE). The black dots represent the mean survival measured with ± SE error
464 bars. The linear model prediction of survival is shown by the blue line and the 95 % C.I.
465 by the dotted black lines.
466
467 The effects of exposure to the seven-level elevated $pCO_2$ gradient on mean lobster
468 survivorship are presented in Fig. 3 and summarised in Table 2. All mortalities recorded
469 were a result of mortality during or immediately following the moulting process of stage
470 IV to stage V. Stage V lobster juvenile's mean survival was highest at the 600 $\mu$atm $pCO_2$
471 level and lowest at the 1200 $\mu$atm $pCO_2$ level (60.52 ± 8.04 and 39.02 ± 8.08 %,
472 respectively, see Table 2). Mean survival decreased significantly with increasing $pCO_2$ ($Z$
473 $_{1, 264}$ = – 2.043, $P$ = 0.041), which was best described by a linear regression (Fig. 3).

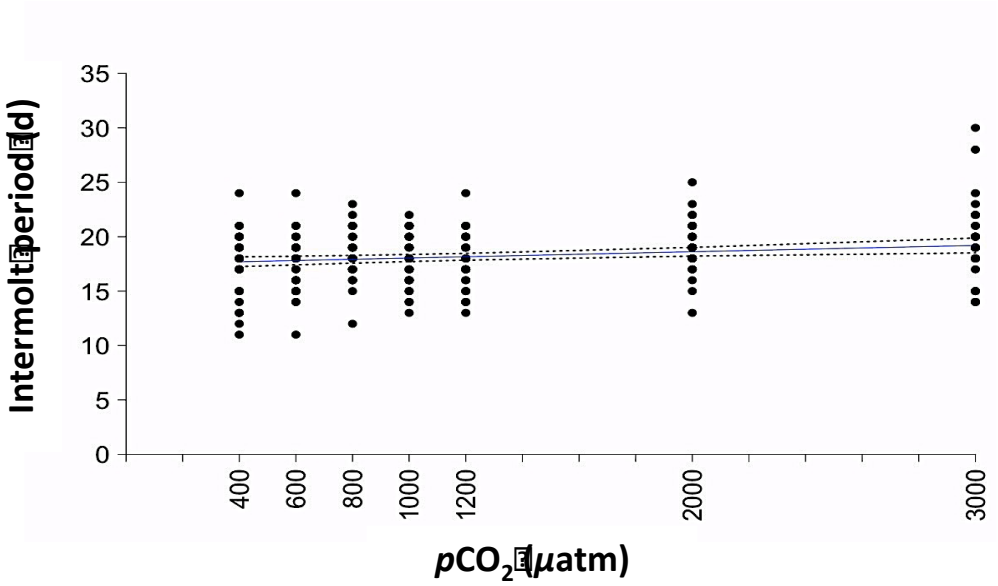


**Fig. 4.** Relationship between seawater $pCO_2$ levels ($\mu$atm) and intermoult period (IP, days) in stage V American lobsters. The black dots represent individual IP recorded across $pCO_2$ levels. The linear model prediction is shown by the blue line and the 95 % C.I. of the model by the dotted black lines.

Stage V Intermolt Period (IP) (mean ± SE, Fig. 2, Table 2) was found to be the shortest at the 400 $\mu$atm control $pCO_2$, and increased significantly with increasing $pCO_2$ ($F_{1, 259}$ = 9.928 $P$ = 0.002, $R^2$ = 0.037, Adjusted-$R^2$ = 0.033), which was best described by a linear regression (Fig. 4).

### 3.3 Feeding rates and routine metabolic rates

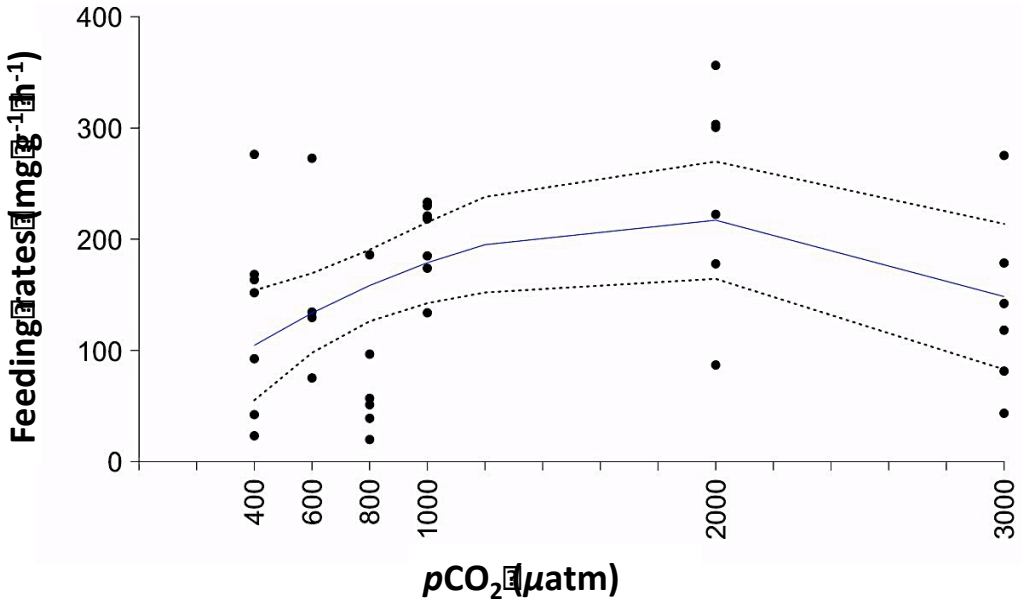


**Fig. 5.** Relationship between seawater $pCO_2$ levels ($\mu$atm) and feeding rates (FR, mg $g^{-1}$ $h^{-1}$) of stage V American lobsters. The black dots represent individual FR measured across the $pCO_2$ gradient investigated. The 2nd order polynomial model prediction of FR is shown by the blue line and the 95 % C.I. of the model by the dotted black lines.

The mean feeding rate (FR) of stage V lobsters (Mean ± SE, Fig. 5, Table 2) was significantly affected across the $pCO_2$ gradient investigated ($F_{1, 35}$ = 3.376, $P$ = 0.046, $R^2$ = 0.170, Adjusted-$R^2$ = 0.120), having the lowest rates at the 800 $\mu$atm $pCO_2$ level and highest at the 2000 $\mu$atm $pCO_2$ level: 74.93 ± 24.50, 241.19 ± 40.33 mg $g^{-1}$ $h^{-1}$, respectively. The relationship between seawater $pCO_2$ and FR was best described by a second order polynomial regression (Fig. 5). In more detail, FR first increased with increasing seawater $pCO_2$ between 400 and 1 000 $\mu$atm followed by a plateau between 1000 and 2000 $\mu$atm, and finally FR decreased between 2 000 and 3 000 $\mu$atm.

Mean routine metabolic rates (RMR) of stage V juvenile lobsters (Table 2) ranged between 1.0647 ± 0.185 $\mu$mol $O_2$ $h^{-1}$ under control conditions and 0.615 ± 0.141 $\mu$mol $O_2$ $h^{-1}$ at 3 000 $\mu$atm of seawater $pCO_2$. However, no significant effect of seawater $pCO_2$ on this variable was detected ($F_{1, 47}$ = 1.580, $P$ = 0.215, $R^2$ = 0.166, Adjusted-$R^2$ = 0.109).

**3.4 Morphometrics**

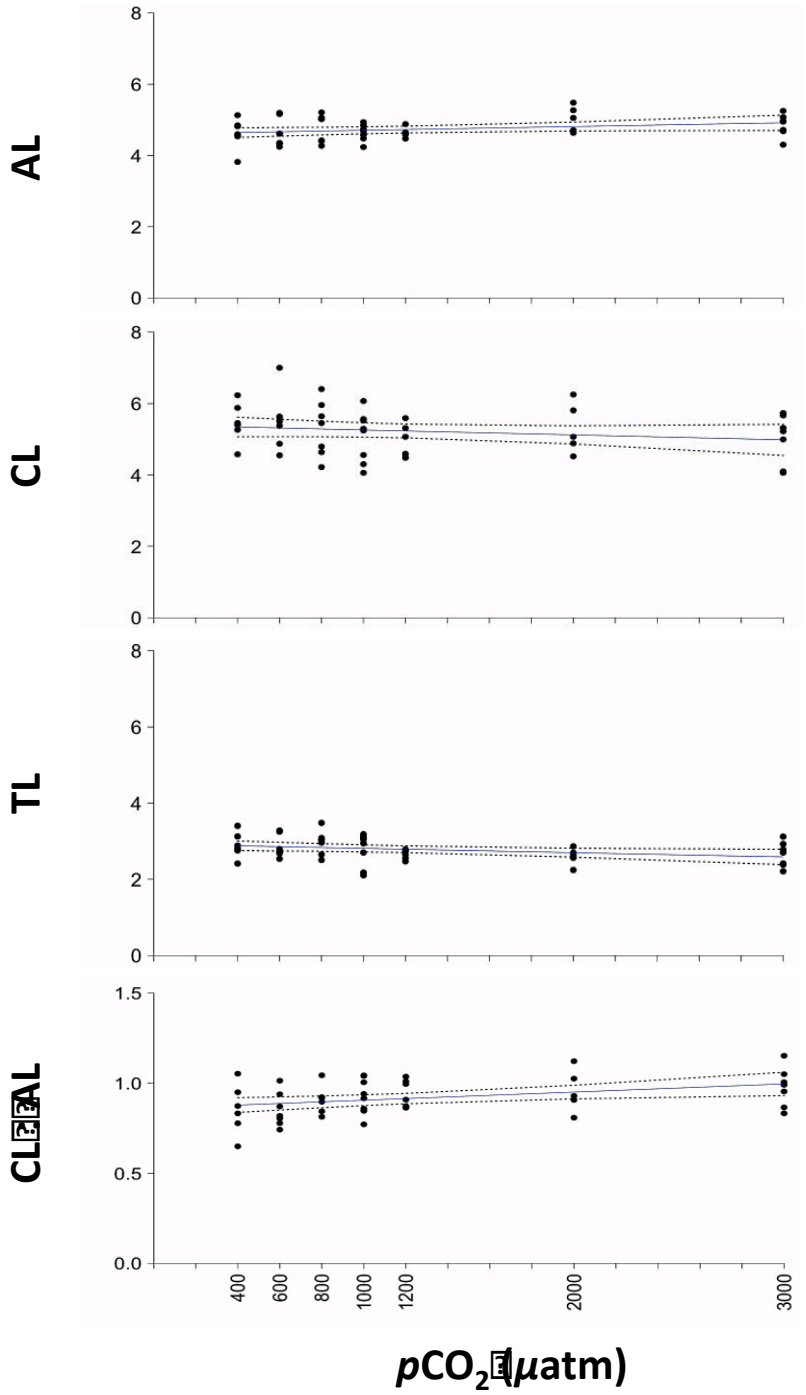


**Fig. 6.** Relationships between seawater $pCO_2$ ($\mu$atm) and abdomen length (AL), cephalothorax length (CL), telson length (TL) in mm, and cephalothorax-abdomen length ratio (CL:AL) for stage V American lobsters. The black dots represent the morphometric trait lengths (mm) for individuals across the seawater $pCO_2$ gradient tested. The linear model prediction of the morphometric traits and ratio are shown by the blue line and the 95 % C.I. of the model by the dotted black lines.

Mean morphological trait of the juvenile lobsters showed significant effects of $pCO_2$ level for the abdomen length, decreasing with $pCO_2$ level ($F_{1,45}$ = 7.605, $P$ = 0.00851, $R^2$ = 0.820, Adjusted-$R^2$ = 0.811), for cephalothorax length (CL), increasing steadily with $pCO_2$ level ($F_{1,45}$ = 6.446, $P$ = 0.0148, $R^2$ = 0.512, Adjusted-$R^2$ = 0.489), and for telson length (TL), decreasing with $pCO_2$ level ($F_{1,45}$ = 0.133, $P$ = 0.00271, $R^2$ = 0.602, Adjusted-$R^2$ = 0.584). These relationships were each best described by a linear regression (Fig. 6). Stage V lobster juvenile mean cephalothorax-abdomen lenght ratio (CL:AL) increased with increasing $pCO_2$ level ($F_{1,45}$ = 6.916, $P$ = 0.0117, $R^2$ = 0.136, Adjusted-$R^2$ = 0.116), which was best described by a linear regression (Fig. 6).

### 3.5 Carapace mineral content

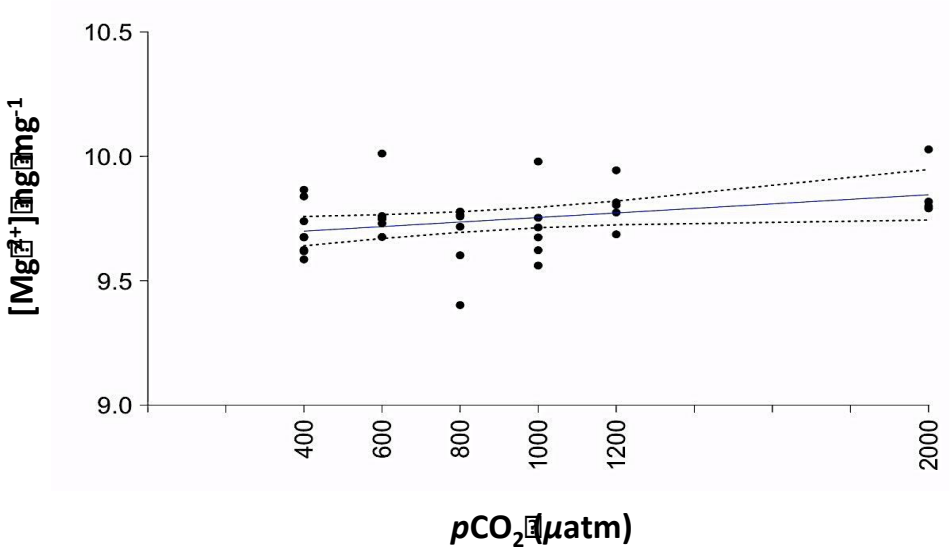


**Fig. 7.** Relationship between seawater $pCO_2$ ($\mu$atm) and on carapace [$Mg^{2+}$] (ng $mg^{-1}$) in stage V American lobsters. The linear model prediction for [$Mg^{2+}$] is shown by the blue line and the 95 % C.I. of the model by the dotted black lines.

Due to sample contamination at the 3 000 $\mu$atm $pCO_2$ level during transportation, enzyme activities were not measured at this level. Of the mineral component tests, only [$Mg^{2+}$] increased significantly with increasing $pCO_2$ ($F_{1,35}$ = 4.611, $P$ = 0.040, $R^2$ = 0.174, Adjusted-$R^2$ = 0.123), which was best described by a linear regression (Fig. 7). Stage V lobsters' mean [$Mg^{2+}$] were lowest at the 800 $\mu$atm $pCO_2$ level and reached a maximum at the 2 000 $\mu$atm $pCO_2$ level (Table 2). In addition, there were no significant differences in carapace ([$Sr^{2+}$], [$Ca^{2+}$], [$Na^{+}$], and [$K^{+}$] quantifications, nor for the [$Ca^{2+}$] : [$Mg^{2+}$] at the different $pCO_2$ tested.

### 3.6 Electron Transport System (ETS), Lactate Dehydrogenase (LDH), and ETS:LDH

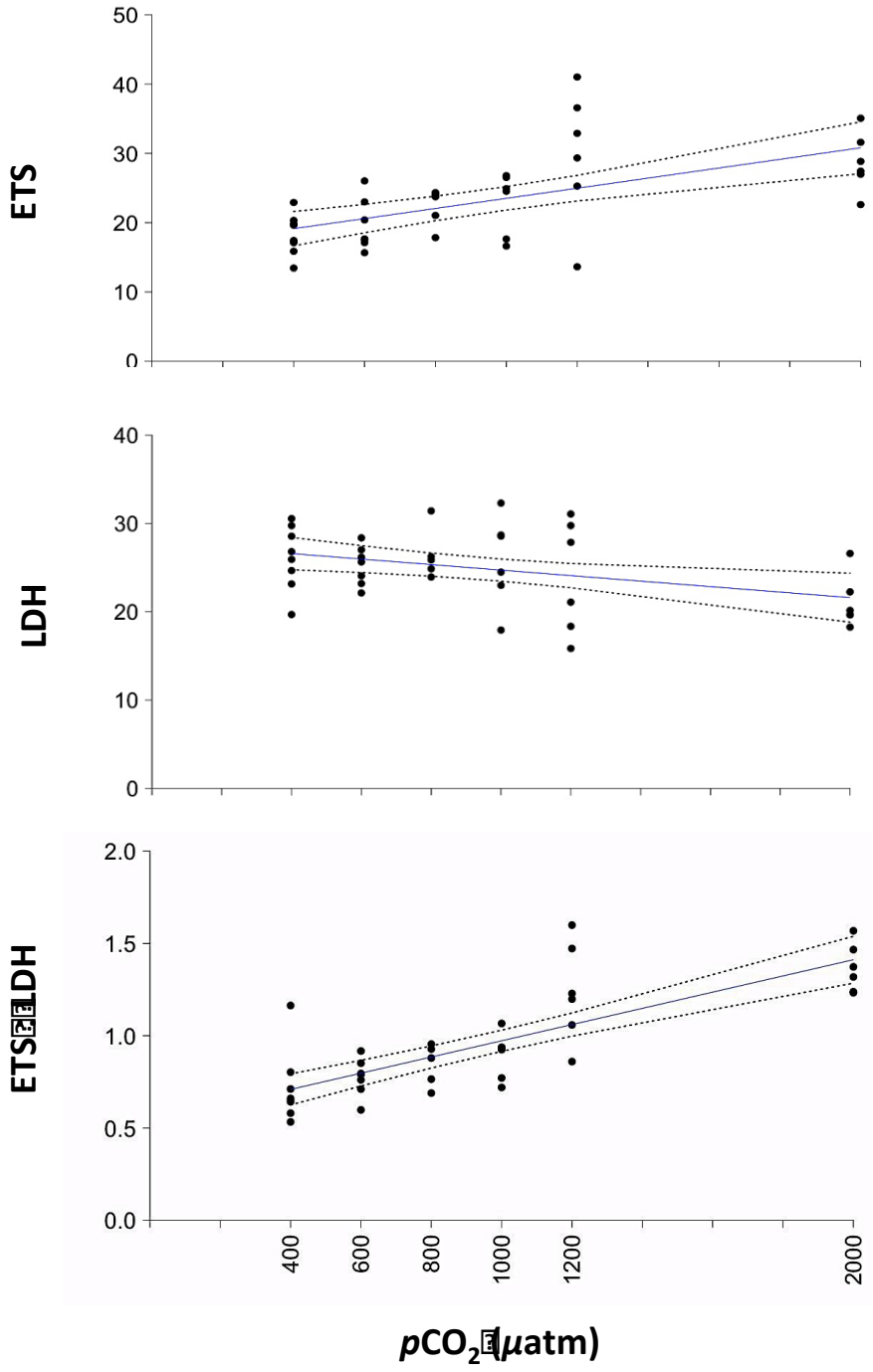


**Fig. 8.** Relationship between seawater $pCO_2$ ($\mu$atm) and the enzyme activity (U mg protein$^{-1}$) of the electron transport system (ETS), lactate dehydrogenase (LDH), and the ETS-LDH ratio (ETS:LDH) in stage V American lobsters. The black dots represent the ETS

544 and LDH activity and the ratio for each individual across $pCO_2$ levels. The linear model
545 prediction for the measure of cellular energy consumption is shown by the blue line
546 (ETS, LDH, ETS:LDH prediction ~ $pCO_2$ ) and the 95 % C.I. of the model by the dotted
547 black lines.
548
549 Due to sample contamination at the 3 000 $\mu$atm $pCO_2$ level during transportation,
550 enzyme activities were not measured at this level. Stage V lobster mean ETS activity was
551 the lowest at the 400 $\mu$atm control $pCO_2$ level and highest at the 1 200 $\mu$atm $pCO_2$ level
552 (18.3 ± 1.05, 29.8 ± 3.93 U mg protein$^{-1}$, respectively). The ETS activity increased
553 significantly with $pCO_2$ level ($F_{1,36}$ = 19.488, $P$ < 0.001, $R^2$ = 0.351, Adjusted-$R^2$ = 0.333,
554 Fig. 8). Stage V lobster juvenile mean LDH activity was the highest at the 400 $\mu$atm
555 control $pCO_2$ level and highest at the 2 000 $\mu$atm $pCO_2$ level (26.1 ± 1.28, 21.1 ± 1.22 U
556 mg protein$^{-1}$, respectively). The LDH activity decreased significantly ($F_{1,36}$ = 7.219, $P$ =
557 0.0109, $R^2$ = 0.167, Adjusted-$R^2$ = 0.144, Fig. 6). ETS:LDH was the smallest at the control
558 $pCO_2$ level at 0.718 ± 0.07 (see Table 2), and highest at the highest $pCO_2$ level measured
559 at 1.36 ± 0.05, increasing significantly with $pCO_2$ level ($F_{1,36}$ = 59.809, $P$ < 0.001, $R^2$ =
560 0.624, Adjusted-$R^2$ = 0.614, Fig. 8).
561
562

## 4. DISCUSSION

Life history and physiological responses of stage V juvenile American lobsters, an ecologically and economically important marine species with a complex life cycle, was examined for the first time under a seven-level $pCO_2$ gradient ranging from 400 to 3 000 $\mu$atm ($pH_T$: 8.1 – 7.1). The negative impacts of the exposure to increasing seawater $pCO_2$ on life history and physiological traits of juvenile lobsters are largely linear. In addition, the observed relationships between increasing $pCO_2$ level and survival, development, and morphology appear to be explained by the observed increase in aerobic mitochondrial respiration, as well as changes in feeding rates (FR). We discuss the potential implications for future benthic recruitment in the American lobster under ocean acidification (OA), as well as under extreme $pCO_2$ events which will occur more frequently in coastal areas in the future ocean, including the potential leakages from carbon capture storages (CCS). We conclude on the potential implications of the reduced energetic capacity of the juvenile lobsters under future elevated $pCO_2$ reported here for the viability of the lobsters populations and the connected fishing industry.

### 4.1 Impact of increasing seawater $pCO_2$ level on life history traits

The predicted value (blue line) for lobsters' survival decreased by 24 % between the 800 and 3 000 $\mu$atm $pCO_2$ conditions. Reduced juvenile survival is a common occurrence among early life stages of crustaceans exposed to elevated $pCO_2$ such as the European lobster, *H. gammarus*, (Small *et al.,* 2016), the porcelain crab, *P. cinctipes* (Carter *et al.,* 2013; Ceballos-Osuna *et al.,* 2013), the edible crab, *Cancer pagurus* (Metzger *et al.,* 2007), and the blue king crab *Paralithodes platypus* (Long *et al.,* 2017). Stage V juveniles in this study appear to be most sensitive to stage-long exposure to seawater $pCO_2$ levels that exceed OA predictions. Similarly, post-larval stages reared under OA conditions (750 $\mu$atm) displayed a reduction in survival of 18 % (Waller *et al.,* 2016), which is best explained by the effects of OA on transition metamorphic stage between the last larval pelagic phase stage and the benthic post-larval stage. This decrease in survival rate with the $pCO_2$ increase is correlated to a prolonged period of vulnerability for the few surviving juveniles at high $pCO_2$ levels, with a prolonged intermoult period (IP) by up to approx. two days at the highest $pCO_2$. This extension of the duration of the stage IV phase has also been observed in juveniles of the American lobsters and might highlight increasing physiological challenges to prepare for the moult to stage V (McLean *et al*., 2016). In the wild, this increase of the stage IV IP may extend the time that post-larvae swim up in the water column and down to the sea bottom, exposing them to broader abiotic fluctuations, and increasing the mismatches between favourable environmental conditions and suitable substratum for recruitment, as well as predation risk in the water column.

While the total length of the juveniles remained unaffected by the exposure to increasing seawater $pCO_2$, the proportions of measured morphological traits differed significantly, although slightly, with increasing seawater $pCO_2$. Similarly, the carapace size of the juvenile blue king crab, *P. platypus*, was little affected by exposure to OA seawater $pCO_2$ levels, displaying slightly smaller carapace size at 1 600 $\mu$atm $pCO_2$

conditions at specific developmental stages (Long *et al., 2017*). Another study on juvenile American lobsters indicated that juvenile lobsters are smaller and grow at a slightly slower rate in early development at elevated $pCO_2$ conditions (McLean *et al.,* 2016). However, comparing the juvenile lobsters from this study in the 3 000 $pCO_2$ treatment to those in the control conditions, their carapace and their total length were larger and smaller respectively. The thorax is the region where critical structures are located, such as the respiratory and circulatory systems, the primary digestive system, the central nervous system, as well as the reproductive organs (Bliss, 1983). Because the thorax holds a major part of these fundamental systems and organs, it is an important region for respiration and gas exchange functions that help to maintain acid-base balance, as well as for digestion, reproduction, and nervous system functions that are also imperative for the species survival. Furthermore, the abdomen and telson are important structures for swimming and manoeuvrability (Factor, 1995). A reduction in the length of the latter two structures relative to enlarging the thorax may represent a trade-off in morphological proportions, perhaps in order to increase the gas-exchange capacity by enlarging the area responsible for maintaining adequate respiratory and cardiovascular functions, and thus enabling a more effective maintenance of internal homeostasis (Bliss, 1983). In fact, the juveniles of this study were able to maintain unchanged metabolic rates across the entire $pCO_2$ gradient tested, which may be helped by the allocation of energy towards enlarging the thorax relative to the abdomen and telson at high $pCO_2$ levels: see also section below on metabolic rates. Besides the compensatory effects of the enlarged thorax, shortening the abdomen and telson could have negative functional repercussions (e.g. on predator evasion) from an ecological point of view. A reduced abdomen length may also have important economical implication for the lobster fisheries, if these morphological patterns persist into adulthood.

The mineral composition of the carapace of the juveniles did not drastically change (Fig. 5), as only $[Mg^{2+}]$ content linearly increased with exposure to increasing $pCO_2$. Small *et al.* (2010) reported a similar response in carapace $[Mg^{2+}]$ for the chelae of adult velvet swimming crabs, *Necora puber*. It appears that such an increase in carapace $[Mg^{2+}]$ might make the carapace potentially more susceptible to dissolution under future elevated $pCO_2$ (Ries, 2011), leading to negative impacts on carapace structure and hardness, but also ventilation, food acquisition, mobility and defense of juveniles of the *H. americanus*. Furthermore, and in contrast with our results, the European lobster exposure to elevated $pCO_2$ has been associated with a decrease in carapace $[Mg^{2+}]$ in both larvae and juveniles (Agnalt *et al.,* 2013; Arnold *et al.,* 2009; Small *et al.,* 2016). This difference in the mineralogical responses to elevated $pCO_2$ further support the idea that species-specific differences exist for the impacts to future OA and CCS leakages in phylogenetically closely related species (e.g. Calosi *et al.* 2013; Seibel *et al*., 2012).

Altogether, carapace structure and mineralisation are not strongly affected by the exposure to elevated $pCO_2$ conditions and the body proportion favouring the maintenance of the carapace length relative to the abdomen length may be expected to

enable the maintenance of adequate respiratory and cardiovascular functions, and thus appropriate metabolic rates. However, the significant decrease in survival and extension of the IP along with the increase in $pCO_2$, both considering OA and CCS scenarios, show patterns of vulnerability in life history traits apparently being explained by underlying physiological impacts on cellular metabolism and energetics.

### 4.2 Impact of increasing seawater $pCO_2$ on metabolism and feeding rates

Routine metabolic rates (RMR) were maintained across the seven-level seawater $pCO_2$ gradient tested. The ability to maintain RMR under elevated $pCO_2$ was also reported for larvae of the American lobster (Waller *et al.,* 2016), larvae of the Norway lobster, *Nephrops norvegicus* (Wood *et al.,* 2014), and juveniles of the porcelain crab, *Petrolisthes cinctipes* (Carter *et al.,* 2013) when exposed to future OA conditions. This ability might be linked to the increase in cephalothorax length, allowing the lobster to maintain their respiratory capacity in high $pCO_2$ conditions. Differently from RMR, the impact of increasing seawater $pCO_2$ on metabolism appears to cause variable behavioural effects on feeding rates (FR). Initially, FR increased with increasing $pCO_2$, which was already observed in juvenile American lobsters under exposure to end-century $pCO_2$ scenarios (Waller *et al.,* 2016). Under levels of $pCO_2$ mimicking CCS leakages, in our study FR decreased towards normal levels, an effect also reported for the juveniles of the European lobster (Small *et al.,* 2016). Here, reducing FR under CCS conditions to the level observed at control conditions can be explained either by the fact that nutritional requirements are satisfied, or that energetic demand exceeds the energy availability at elevated $pCO_2$ levels, limiting digestive ability and preventing changes in feeding behaviour. It is possible that available energy is allocated to mechanisms and behaviours responsible for maintaining RMR and FR at elevated $pCO_2$ levels, at the cost of other processes.

Juvenile lobster exposure to increasing $pCO_2$ levels elicited a strong positive linear response on the enzymatic activity in the mitochondrial electron transport system (ETS) and a slightly weaker negative linear response on the lactate dehydrogenase (LDH) activity. In marine species, ETS activity is often used as a proxy for energy consumption in aerobic respiration (Tonn *et al*., 2016), and LDH is often used as a proxy for anaerobic glycolytic capacity (Kaplan and Pesce, 1996). Thus, the significant increase in ETS and decrease in LDH observed here with increasing $pCO_2$ are indicative of reorganisation of energy metabolism apparatus in OA and CCS conditions. This is even clearer when looking at the strong positive linear response of the ETS/LDH ratio, which suggests that mitochondrial responses are taking place during the stage-long acclimation of juvenile lobsters to elevated $pCO_2$ levels.
These results could arise from mito-hormetic reactions in stressful conditions (Yun and Finkel, 2014), brought on by differential gene expression at elevated $pCO_2$ levels (Ristow and Schmeisser, 2014; Schulz, 2007). In such conditions, mitochondrial oxidative stress can trigger cytosolic signalling pathways that culminate in the multiplication and increment of mitochondrial content in order to meet the energy requirement imposed by the exposure to elevated $pCO_2$ (Valero, 2014). However, this hypothesis requires

695 further validation *via* the examination on the impacts of elevated $pCO_2$ levels on
696 oxidative stress: production rate of ROS and markers of oxidative stress as products of
697 peroxidation of lipids, carbonylation of proteins or oxidation of nucleotides (8-
698 oxoguanosine). Additionally, these measurements should be conducted with parallel
699 tests of mtDNA content, which is expected to increase as a response to metabolic and
700 oxidative stress.
701 In a similar study that examined the effects of an end-century OA $pCO_2$ level (710 $\mu$atm)
702 on the European lobster's larval stages, LDH and ETS activity were also measured as
703 proxies for anaerobic energetic metabolism and energy expenditure, respectively (Rato
704 *et al*., 2017). Although the average LDH and ETS concentrations were similar and highly
705 variable in control and OA conditions, it was presumed that energetic impacts might still
706 have occurred in response to OA conditions, explaining the growth reduction and the
707 potential increase in oxidative stress in the specimens (Rato *et al*., 2017). Like the
708 European lobster larvae, the morphological changes in the abdomen, cephalothorax,
709 and telson lengths of the juvenile lobsters in this study could also be related to energetic
710 trade-offs due to an increase in energy demand at the mitochondrial level.
711 OA and CCS impacts detected on the mitochondrial processes in the juvenile lobsters of
712 this study may explain other observed impacts, especially on the maintenance of RMR
713 with increasing $pCO_2$. For instance, it was suggested that metabolic energy reallocation
714 towards physiological functions at OA $pCO_2$ levels (1 030 and 1 450 $\mu$atm) could explain
715 smaller larval sizes in the purple sea urchin, *Strongylocentrotus purpuratus* (Matson *et*
716 *al*., 2015). In the present study, the observed increase in the juvenile lobsters ETS
717 activity (i.e. aerobic metabolism), indicates an increase in mitochondrial energetic
718 capacity under elevated $pCO_2$ levels. In the present study, the observed increase in the
719 juvenile lobsters ETS activity (i.e. aerobic metabolism), indicates an increase in
720 mitochondrial energetic capacity under elevated $pCO_2$ levels, perhaps in order to
721 allocate enough energy to physiological functions for repair and maintenance at a higher
722 level of complexity.
723 Together with negative impacts on the life history traits with increasing seawater $pCO_2$
724 levels, the cost of mito-hormesis seems to be necessary for maintaining two main
725 processes in stage V juvenile lobsters: RMR levels and carapace mineral content.
726 Unfortunately, beyond intermediate $pCO_2$ levels used in this study, this response may be
727 too energetically expensive, becoming lethal for the majority of stage V juvenile lobsters
728 at the most elevated $pCO_2$ levels.
729
730 **4.3 Integrating laboratory biological responses to *in situ In situ* lobsters habitat**
731 **physical and chemical profiles**
732 The vertical profiles throughout 2012 and 2015 (Fig. 8), and more specifically between
733 the months of May and November (Fig. 7), indicate that stage IV lobster post-larvae
734 encounter higher $pCO_2$ values as they naturally swim to the benthos in order to settle
735 for juvenile recruitment. Following the post-larval settlement stage, it is apparent that
736 newly moulted juvenile lobsters in the benthos may be subject to $pCO_2$ values that are
737 currently already more elevated than the IPCC $pCO_2$ predictions for 2050 in the open

738 ocean (2014, RCP 2.6, RCP 4.5, RCP 6.0). It is possible that the effects of the first levels of
739 the $pCO_2$ used in this study are less noticeable on the life history and physiology of the
740 specimens because such $pCO_2$ values (between 400 and 800 $\mu$atm) are already
741 experienced at this life-stage in the wild. Therefore, the individuals may be already
742 adapted to these $pCO_2$ levels at the post-larval and juvenile phase in development. The
743 $pCO_2$ and omega values become biologically harsher for the crustacean with depth in
744 the water column with respect to the acid-base regulation capacity (Whitely, 2011), and
745 consequently, on the energy budget and metabolism (Carter *et al*., 2013). In the future,
746 the potential effects of low pH / elevated $pCO_2$ levels will be progressively enhanced
747 with time for the American lobsters, as elevated $pCO_2$ levels become a prominent
748 chemical threat.
749
750 **4.4 Conclusion**
751 In conclusion, increasing seawater $pCO_2$ has mostly negative implications on juvenile
752 American lobsters, with the most serious impacts on energetic capacity and allocation,
753 as well as decreased survival rates. Other impacts of elevated $pCO_2$ levels include slower
754 development, altered feeding behaviour, and a significant transformation of the body
755 proportions and carapace mineral content. These are likely compensatory effects to
756 attempt to sustain fundamental mechanisms necessary for survival. Relative to OA, CCS
757 leakage implications on juvenile lobsters display the most serious biological threats,
758 foreshadowing a high-risk potential on early lobster life history if CCS systems were to
759 be constructed in the North-West Atlantic shores near American lobsters habitats. By
760 preventing the successful completion of consecutive developmental phase (Byrne,
761 2013), the negative impacts of stage-long exposure to increasing seawater $pCO_2$ on
762 juvenile lobster survival may threaten the species recruitment success over time. Thus,
763 the implication of the exposure to OA and CCS leakages on lobster juveniles may
764 negatively reduce future population abundances along American and Canadian shores
765 especially in coastal environments experiencing drastic drops in pH in the water column.
766 By incorporating the potential of low pH impacts on American lobster recruitment, it
767 may be possible to better predict population variability and pH vulnerability hot-spots
768 along the North-West Atlantic coast. This could significantly improve the future plans for
769 stock management projects and better prepare local fishermen for the future of this
770 crucial Canadian crustacean.
771

772 **Acknowledgements**: We wish to thank Véronique Desrosiers, Mathieu Babin, Jonathan
773 Day, Jocelyn Leger, Steve Neil, Steve Punshen, Lara Cooper, and Andrew Cooper for
774 technical help and/or useful discussions. Coastal Zones Research Institute (*CZRI)* for
775 providing juvenile lobsters and technical support for proper specimen husbandry.
776
777 **Funding**: This work was supported by the MEOPAR I-CAP Ocean Acidification awarded to
778 DD, KAS and PC and from DFO's ACCASP and Partnership programs to KAS. KMC was
779 supported by MEOPAR and a NSERC industrial Undergraduate Student Research Award
780 (IUSRA) (reference # 481258). FN was supported by MEOPAR funding and a QCBS

781 Excellence Fellowship (199173). SP was supported by a NSERC Undergraduate Student
782 Research Award (USRA) (reference # 440371). PUB and PC were supported by a Natural
783 Sciences and Engineering Research Council of Canada (NSERC) Discovery Program grant
784 (RGPIN 155926 and RGPIN-2015-06500 respectively).
785
786 **Competing interests**: The authors confirmed that there are no competing interests.

787

788

## References


**Addison, J. T. and Bannister, R. C. A.** (2014). Re-Stocking and Enhancement of Clawed Lobster Stocks : A Review. *Crustaceana*. **67** (2), 131–155.

**Agnalt, A. L., Grefsrud, E. S., Farestveit, E., Larsen, M. and Keulder, F.** (2013). Deformities in larvae and juvenile European lobster (Homarus gammarus) exposed to lower pH at two different temperatures. *Biogeosciences.* **10**, 7883–7895.

**Arnberg, M., Calosi, P., Spicer, J. I., Tandberg, A. H. S., Nilsen, M., Westerlund, S. and Bechmann, R. K.** (2013). Elevated temperature elicits greater effects than decreased pH on the development, feeding and metabolism of northern shrimp (Pandalus borealis) larvae. *Mar. Biol.* **160**, 2037–2048.

**Arnold, K. E., Findlay, H. S., Spicer, J. I., Daniels, C. L. and Boothroyd, D.** (2009). Effect of $CO_2$-related acidification on aspects of the larval development of the European lobster Homarus gammarus (L.). *Biogeosci. Discuss.* **6**, 3087-3107.

**Bannister, R. C. A., and J. T. Addison.** (1998). Enhancing lobster stocks: A review of recent European methods, results, and future prospects. *Bull. Mar. Sci.* **62** (2), 369-387.

**Blackford J, Jones N, Proctor R, Holt J, Widdicombe S, Lowe D, Rees A.** (2009) An initial assessment of the potential environmental impact of $CO_2$ escape from marine carbon capture and storage systems. *Pro.c Inst. Mech. Eng. A. J. Power Energy.* **223**, 269–280

**Blackford, J., Bull, J. M., Cevatoglu, M., Connelly, D., Hauton, C., James, R. H., Lichtschlag, A., Stahl, H., Widdicombe, S. and Wright, I. C.** (2015). Marine baseline and monitoring strategies for carbon dioxide capture and storage (CCS). *Int. J. Greenh. Gas Control* **38**, 221–229.

**Blackford, J., Stahl H., Bull, J.M., Bergès, B.J.P., Cevatoglu, M., Lichtschlag, A., Connelly, D., James, R.H., Kita, J., Long, D., Naylor, M., Shitashima, K., Smith, D., Taylor, P., Wright, I., Akhurst, M., Chen, B., Gernon, T.M., Hauton, C., Hayashi, M., Kaieda, H., Leighton, T.G., Sato, T., Sayer, M.D.J., Suzumura, M., Tait, K., Vardy, M.E., White, P.R., Widdicombe, S.** (2014). Detection and impacts of leakage from sub-seafloor carbon dioxide storage. *Nat. Clim. Change.* http://dx.doi.org/10.1038/nclimate2381

**Blackford, J., Stahl, H., Kita, J. and Sato, T.** (2015). Preface to the QICS special issue. *Int. J. Greenh. Gas Control* **38**, 1.

**Blackford, J.C., Jones, N., Proctor, R., Holt, J.** (2008). Regional scale impacts of distinct

824 $CO_2$ additions in the North Sea. *Mar. Pollut. Bull.* **56**, 1461–1468.

825 **Bliss, D. E.** 1983. The Biology of Crustacea: Internal Anatomy and Physiological
826 Regulation. Academic Press, Inc. London Ltd, 24/28 Oval Road, London NW1 7DX. **5**,
827 1-41.

828 **Byrne, M.** (2011). Impact of ocean warming and ocean acidification on marine
829 invertebrate life history stages: vulnerabilities and potential for persistence in a
830 changing ocean. *Oceanogr. Mar. Biol. An Annu. Rev.* **49**, 1–42.

831 **Byrne, M. and Przeslawki, R.** (2013). Multistressor impacts of warming and acidification
832 on marine invertebrates' life histories. *Integr. Comp. Biol.* **53** (4), 582-596.
833
834 **Calosi P., Turner L.M., Hawkins M., Bertolini C., Nightingale G., Truebano M., Spicer J.I.**
835 (2013) Multiple physiological responses to multiple environmental challenges: an
836 individual response. *Integr. Comp. Biol.* **53**, 660–670

837 **Carter H.A., Ceballos-Osuna L., Miller N.A., and Stillman J. H.** (2013). Impact of ocean
838 acidification on metabolism and energetics during early life stages of the intertidal
839 porcelain crab Petrolisthes cinctipes. *J. Exp. Biol.* **216**, 1412–22.

840 **Castro K. M., J. S. Cobb, R. A. Wahle, and J. Catena.** 2001. Habitat addition and stock
841 enhancement for American lobster, *Homarus americanus*. *Mar. Freshw. Res.* **52**,
842 1253-1261.

843 **Ceballos-Osuna, L., Carter, H. A., Miller, N. A. and Stillman, J. H.** (2013). Effects of
844 ocean acidification on early life-history stages of the intertidal porcelain crab
845 Petrolisthes cinctipes. *J. Exp. Biol.* **216**, 1405–1411.

846 **Cheung, W. W. L., Lam, V. W. Y., Sarmiento, J. L., Kearney, K., Watson, R., Zeller, D.,**
847 **Pauly, D.** (2010). Large scale redistribution of maximum fisheries catch potential in
848 the global ocean under climate change. *Glob. Change Biol*. **16**, 24-35.
849
850 **Christen, N., Calosi, P., McNeill, C. L. & Widdicombe, S.** (2013). Structural and
851 functional vulnerability to elevated pCO2 in marine benthic communities. *Mar. Biol.*
852 **160**, 2113–2128.
853
854 **Chiasson, M., Miron, G., Daoud, D., Mallet, M. D.** (2015). Effect of temperture on the
855 behaviour of stage IV American lobster (Homarus americanus) larvae. *J. Shell. Res.*
856 **34** (2), 545-554. https://doi.org/10.2983/035.034.0239
857
858 **Comeau, M. J., M. Hanson, M. Mallet, and F. Savoie.** 2004. *Stock status of the American*
859 *lobster, Homarus amerivcanus, in the Lobster Fishing Area 25. Department of*

860 *Fisheries and Oceans Canadian Scientific Advisory Committee.* Research document
861 2004/054. 70 pp.
862

863 **Daoud, D., Fairchild, W. L., Comeau, M., Bruneau, B., Mallet, M. D., Jackman, P. M.,**
864 **Benhalima, K., Berillis, P. and Mente, E.** (2014). Impact of an Acute Sublethal
865 Exposure of Endosulfan on Early Juvenile Lobster (Homarus americanus). *Aquat. Sci.*
866 *Technol.* **2**, 14.

867 **Dickson, A. G., Sabine, C. L., Christian, J. R.** 2007**.** Guide to best practices for ocean CO2
868 measurements. PICES Special Publication **3**, 191.
869
870 **Donohue P. J. C., Calosi, P., Bates, A. H., Laverock, B., Rastrick, S., Mark, F., C., Strobel,**
871 **A., Widdocombe, S.** (2012). Impact of exposure to elevated pCO2 on the physiology
872 and behaviour of an important ecosystem engineer, the burrowing shrimp
873 Upogebia deltaura. *Aquat. Biol.* **15**, 73-86.
874

875 **Duarte, C., I. Hendriks, T. Moore, Y. Olsen, A. Steckbauer, L. Ramajo, J. Carstensen, J.**
876 **Trotter, and M. McCulloch.** 2013. Is ocean acidification an open-ocean syndrome?
877 Understanding anthropogenic impacts on seawater pH. *Estuaries and Coasts*. **36**,
878 221-236

879 **Drinkwater, K. F., Tremblay, M. J., Comeau, M.** (2005). The influence of wind and
880 temperature on the catch rate of the American lobster (Homarus americanus)
881 during spring fisheries off eastern Canada. *Fish. Oceanogr.* **15** (2), 150-165.
882 https://doi.org/10.1111/j.1365-2419.2005.00349.x

883 **Ekkstrom, J. A., Suatoni, L., Cooley, S. R., Pendleton, L. H., Waldbusser, G. G., Cinner, J.**
884 **E., Ritter, J., Langdon, C., van Hooidonk, R., Gledhill, D., et al.,.** (2015). Vulnerability
885 and adaptation of US shellfisheries to ocean acidification. *Nat. Clim. Chang.* **5**, 207–
886 214.

887 **Factor, J.** (1995) *In* Biology of the Lobster, 1st Edition : Homarus americanus. ISNB :
888 9780122475702. Pp. 528.

889 **Gattuso, J.-P.** (2015). Acidification des océans. *Ocean. Clim.* **1**, 28–30.

890 **Haradsson, C., L. G. Anderson, M. Hassell€ov, S. Hulth, and K. Olsson (1997).** Rapid
891 high-precision potentiometric titration of alkalinity in ocean and sediment pore
892 waters, *Deep Sea Res.*, Part I. **44**, 2031–2044.
893
894 **Hoffman, G., Barry, J. P., Edmunds, P. J., Gates, R. D., Hutchings, D. A., Klinger, T.,**
895 **Sewell, M. A.** (2010). The effects of ocean acidification on calcifying organisms in

marine ecosystems: an organism-ecosystem perspective. **41**, 127-147.

**IPCC** (2014). Climate Change 2014: Synthesis Report. Contribution of Working Groups I, II and III to the Fifth Assessment Report of the Intergovernmental Panel on Climate Change [Core Writing Team, R.K. Pachauri and L.A. Meyer (eds.)]. IPCC, Geneva, Switzerland, 151 pp.

**Incze, L.S., Wahle, R.A.** (1991). Recruitment from pelagic to early benthic phase in lobsters *Homarus americanus*. *Mar. Ecol. Prog. Ser.* **79**, 77–87.

**Incze, L.S., Wahle, R.A., Cobb, J.S.,** 1997. Quantitative relationships between postlarval supply and benthic recruitment in the American lobster, Homarus americanus. *Fish. Bull.* **48**, 729–743.

**Incze, L.S., Wahle, R.A., Palma, A.T.,** 2000. Advection and settlement rates in a benthic invertebrate, recruitment to first benthic stage in *Homarus americanus*. *ICES J. Mar. Sci.* **57**, 430–437.

**Johnson, K. M., A. E. King, Mc Sieburth, M.** (1985), Coulometric TCO2 analyses for marine studies: An introduction. *Mar. Chem.* **16,** 61–82.

**Kaplan, L. A., and Pesce, A. J. (Eds.).** (1996). Clinical Chemistry. Theory, Analysis and Correlation. Mosby-Year Book, Inc., Missouri, pp. 609-610.

**Keppel, E. A., Scrosati, R. A. and Courtenay, S. C.** (2012). Ocean acidification decreases growth and development in American lobster (Homarus americanus) larvae. *J. Northwest Atl. Fish. Sci.* **44**, 61–66.

**Krohn, R.I., G.T. Hermanson, A.K. Mallia, F.H. Gartner, M.D. Provenzano, E.K. Fujimoto, N.M. Goeke, B.J. Olson, D.C. Klenk.** (1985). Measurement of protein using bicinchoninic acid. *Anal. Biochem.* **150** (1), 76–85

**Long, W. C., Van Sant, S. B., Swiney, K. M., Foy, R. J.** (2017). Survival, growth, and morphology of blue king crabs: effect of ocean acidification decreases with exposure time. *ICES J. Mar. Sci*. **74**, 1033-1041.

**Seibel, B. A., Maas, A. E., Dierssen, H. M.** (2011). Energetic plasticity underlies a variable response to ocean acidification in the pteropod, Limacina helicina antarctica. PLoS One, **7**(4), e30464. https://doi.org/10.1371/journal.pone.0030464

**Matson, P. G., Yu, P. C., Sewel, M. A., Hofmann, G. E.** (2012). Development under elevated pCO2 conditions does not affect lipid utilization and protein content in early life-hostory stages of the purple sea urching, Strongylocentrotus purpuratus. *Biol. Bull*. **223**, 312-327.

**McLean, E. L., Katenka, N. V., Seibel, B. A.** Decreased growth and increased shell

933 disease in early benthic phase Homarus americanus in response to elevated CO2.
934 (2018). *Mar. Ecol. Prog. Ser.* **596**, 113-126. https://doi.org/10.3354/meps12586

935 **Metzger, R., Sartoris, F. J., Langenbuch, M. and Pörtner, H. O.** (2007). Influence of
936 elevated CO2 concentrations on thermal tolerance of the edible crab Cancer
937 pagurus. *J. Therm. Biol.* **32**, 144–151.

938 **Orr, J. C., Fabry, V. J., Aumont, O., Bopp, L., Doney, S. C., Feely, R. A., Gnanadesikan,**
939 **A., Gruber, N., Ishida, A., and Joos, F., et al.** (2005). Anthropogenic ocean
940 acidification over the twenty-first century and its impact on calcifying organisms.
941 *Nature*. **437**, 681–686.

942 **Pechenik, J. A.** 1999. On the advantages and disadvantages of larval stages in benthic
943 marine invertebrate life cycles. *Mar. Ecol. Prog. Ser.* **177**, 269-297.

944 **Phelps, J. J. C., Blackford, J. C., Holt, J. T. and Polton, J. A.** (2015). Modelling large-scale
945 CO2 leakages in the North Sea. *Int. J. Greenh. Gas Control.* **38**, 210–220.

946 **Pörtner H.-O., Farrell A. P.** (2008) Physiology and climate change. *Science.* **322**, 690–
947 692.

948 **Pörtner, H. O.** (2008). Ecosystem effects of ocean acidification in times of ocean
949 warming: A physiologist's view. *Mar. Ecol. Prog. Ser.* **373**, 203–217.

950 **Pörtner, H.-O.** (2001) Climate change and temperature-dependent biogeography:
951 oxygen limitation of thermal tolerance in animals. *Naturwissenschaften.* **88**, 137–
952 146

953 **Pörtner, H.-O., D.M. Karl, P.W. Boyd,W.W.L. Cheung, S.E. Lluch-Cota, Y. Nojiri, D.N.**
954 **Schmidt, and P.O. Zavialov,** 2014: Ocean systems. In: Climate Change 2014:
955 Impacts, Adaptation, and Vulnerability. Part A: Global and Sectoral Aspects.
956 Contribution of Working Group II to the Fifth Assessment Report of the
957 Intergovernmental Panel on Climate Change [Field, C.B., V.R. Barros, D.J. Dokken,
958 K.J. Mach, M.D. Mastrandrea, T.E. Bilir, M. Chatterjee, K.L. Ebi, Y.O. Estrada, R.C.
959 Genova, B. Girma, E.S. Kissel, A.N. Levy, S. MacCracken, P.R. Mastrandrea, and
960 L.L.White (eds.)]. Cambridge University Press, Cambridge, United Kingdom and New
961 York, NY, USA, pp. 411-484.

962 **Rastelli, E., Corinaldesi, C., Dell'Anno, A., Amaro, T., Greco, S., Lo Martire, M., Carugati,**
963 **L., Queirós, A. M., Widdicombe, S. and Danovaro, R.** (2016). $CO_2$ leakage from
964 carbon dioxide capture and storage (CCS) systems affects organic matter cycling in
965 surface marine sediments. *Mar. Environ. Res.* **122**, 158–168.

**Rato, L. D., Novais, S. C., Lemos, M. F. L., Alves, L. M. F., Leandro, S. M.** (2017). Homarus gammarus (Crustacea: Decapoda) larvae under an ocean acidification scenario: responses across different levels of biological organization. *Comp. Biochem. Physiol. Part C.* **203**, 29-38.

**Ries, J. B.** (2011). Skeletal mineralogy in a high-$CO_2$ world. *J. Exp. Mar. Bio. Ecol.* **403**, 54–64.

**Ries, J. B., Cohen, A. L. and McCorkle, D. C.** (2009). Marine calcifiers exhibit mixed responses to $CO_2$-induced ocean acidification. *Geology.* **37**, 1131–1134.

**Ristow, M., and Schmeisser, K.** (2014). Mitohormesis: promoting health and lifespan by increased levels of reactive oxygen species (ROS). *Dose-Response*. **12**, 288-341.

**Schulz, T. J., Zarse, K., Voigt, A., Urban, N., Birringer, M., Ristow, M.** (2007). Glucose restriction extends Caenorhabditis elegans life span by inducing mitochondrial respiration and increasing oxidative stress. *Cell Metab.* **6**, 280-293.

**Small, D. P., Calosi, P., Boothroyd, D., Widdicombe Steve and Spicer, J. I.** (2015). Stage-specific changes in physiological and life-history responses to elevated temperature and $pCO_2$ during the larval development of the European lobster Homarus gammarus (L.). *Physiol. Biochem. Zool.* **88**, 494–507.

**Small, D., P., Calosi, P., Boothroyd, D., Widdicombe, S. and Spicer, J. I.** (2016). The sensitivity of the early benthic juvenile stage of the European lobster Homarus gammarus (L.) to elevated $pCO_2$ and temperature. *Mar. Biol.* **163**, 1–12.

**Speakman, J.R., and McQueenie, J.** (1996). Limits to sustained metabolic rate: The link between food intake, basal metabolic rate, and morphology in reproducing mice, Mus musculus. *Physiol. Zool.* **69** (4), 746-769.

**Spicer, J. I. and Eriksson, S. P.** (2003). Does the development of respiratory regulation always accompany the transition from pelagic larvae to benthic fossorial postlarvae in the Norway lobster Nephrops norvegicus (L.)? *J. Exp. Mar. Bio. Ecol.* **295**, 219–243.

**Spicer, J. I., and Gaston, K.** (1999). *In* Physiological Diversity: Ecological Implications.

**Spicer, J. I., Raffo, A. and Widdicombe, S.** (2007). Influence of $CO_2$-related seawater acidification on extracellular acid-base balance in the velvet swimming crab Necora puber. *Mar. Biol.* **151**, 1117–1125.

**Steneck, R. S., Wahle, R. A. and Sainte-Marie, B.** (2013). American lobster dynamics in a brave new ocean [1]. *Can. J. Fish. Aquat. Sci.* **70**, 1612–1624.

**Steneck, R.S., Wilson, C.J. (**2001). Large-scale and long-term spatial and temporal patterns in demography and landings of the American lobster, *Homarus americanus*, in Maine. *Fish. Bull.* **52**, 1303–1320.

**Thibeault M., Blier, P. U., Guderley, H.** (1997). Seasonal variation of muscle metabolic organization in rainbow trout (Oncorhynchus mykiss). *Fish Physiol. Biochem.* **16** (2), 139-155.

**Tonn, N., Novais, S. C., Silva, C. S. E., Morais, H. A., Correia, J. P. S., Lemos, M. F. L. .** (2016). Stress responses of the sea cucumber Holothuria forskali during aquaculture handling and transportation. *Mar. Biol. Res.* **12**, 948-957.

**Turley, C., an Gattusso, J. P.** (2012). Future biological ecosystem impact of ocean of ocean acidification and their socioeconomic-policy implications. *Cur.r Opin. Environ. Sustain.* **4**, 278-286.

**Valero.** (2014). Mitochondrial Biogenesis: pharmacological approaches. *Current Pharmaceutical Design.* **20** (35), 5507-5509.

**Wahle, R. A.** (2003). Revealing stock-recruitment relationships in lobsters and crabs: Is experimental ecology the key? *Fish. Res.* **65**, 3–32.

**Wahle, R., Butler, M., Cockcroft, A. & MacDiarmid, A.** 2011. *Homarus americanus*. The IUCN Red List of Threatened Species 2011: e.T170009A6705155. http://dx.doi.org/10.2305/IUCN.UK.2011-1.RLTS.T170009A6705155.en.

**Wahle, R., Steneck, R., Wahle, R. a and Robert, S.** (1991). Recruitment Habitats and Nursery Grounds of the American Lobster Homarus Americanus : A Demographic Bottleneck? **69**, 231–243.

**Waldbusser, G. G., J. E. Salisbury.** (2013). Ocean Acidification in the coastal zone from an organism's perspective: multiple system parameters, frequency domains, and habitats. Annu. Rev. Mar. Sci. **6**, 221-247, https://doi.org/10.1146/annurev-marine-121211-172238

**Waller, J. D., Wahle, R. A., McVeigh, H. and Fields, D. M.** (2016). Linking rising $pCO_2$ and temperature to the larval development and physiology of the American lobster ( *Homarus americanus* ). *ICES J. Mar. Sci. J. du Cons.* **3**, 154.

**Whiteley, N. M.** (2011). Physiological and ecological responses of crustaceans to ocean acidification. *Mar. Ecol. Prog. Ser.* **430**, 257–271.

**Widdicombe, S. and Spicer, J. I.** (2008). Predicting the impact of ocean acidification on benthic biodiversity: What can animal physiology tell us? *J. Exp. Mar. Bio. Ecol.* **366**, 187–197.

**Widdicombe, S., McNeill, C. L., Stahl, H., Taylor, P., Queiros, A. M., Nunes, J. and Tait, K.** (2015). Impact of sub-seabed CO2 leakage on macrobenthic community structure and diversity. *Int. J. Greenh. Gas Control.* **38**, 182–192.

**Wood, H. L., Spicer, J. I. and Widdicombe, S.** (2008). Ocean acidification may increase calcification rates, but at a cost. *Proc. Biol. Sci.* **275**, 1767–73.

**Yun, J., and Finkel, T.** (2014). Mitohormesis. *Cell Metabolism*. **19**, 757-766.

**Zeebe, R.E., Wolf-Gladrow, D.A.** (2001). CO2 in Seawater: Equilibrium, Kinetics, Isotopes. Third Impression (With Corrections) 2005. Elsevier Ltd, 84 Theobalds Road, London (WC1X *8RR, UK ISBN 0 444 50946 1).